International Journal of Modern Physics E

Azimuthal anisotropy of strange and multi-strange hadrons in isobar collisions at $\sqrt{s_{\rm NN}} = 200$ GeV

Priyanshi Sinha (for the STAR Collaboration)
Indian Institute of Science Education and Research (IISER) Tirupati
Andhra Pradesh, India
priyanshisinha@students.iisertirupati.ac.in

Received Day Month Year
Revised Day Month Year

The objective of relativistic heavy-ion collisions is to create matter under high temperature and high density, called Quark-Gluon Plasma, and study its properties. Strange and multi-strange hadrons have a smaller hadronic cross-section than light hadrons, making them a better probe for comprehending the partonic stage of collisions. In 2018, isobar collisions, $^{96}_{44}$Ru+$^{96}_{44}$Ru and $^{96}_{40}$Zr+$^{96}_{40}$Zr, at $\sqrt{s_{\rm NN}} = 200$ GeV have been performed at RHIC. These collisions effectively minimize the background contribution in the search for the Chiral Magnetic Effect (CME). Flow measurements are quite sensitive to the different deformation characteristics between the two species. A comprehensive elliptic flow (v_2) measurement of strange hadrons gives direct information about the initial spatial anisotropies and helps to understand the CME background. We present the v_2 of K^0_s, Λ, $\bar{\Lambda}$, ϕ, Ξ^-, and $\overline{\Xi}^+$, at mid-rapidity ($|y| < 1.0$) for Ru+Ru and Zr+Zr collisions at $\sqrt{s_{\rm NN}} = 200$ GeV. The measurements of v_2 as a function of centrality and transverse momentum (p_T) are shown. The dependence of v_2 for different colliding systems such as Cu+Cu, Au+Au, and U+U is discussed. The physics implications of such measurements in the context of nuclear deformation in isobars is also discussed.

Keywords: Isobar; elliptic flow; strange.

PACS numbers:

1. Introduction

In 2018, RHIC conducted a dedicated experiment involving involving two isobar species specifically, colliding $^{96}_{44}$Ru+$^{96}_{44}$Ru and $^{96}_{40}$Zr+$^{96}_{40}$Zr, at a center-of-mass energy of $\sqrt{s_{\rm NN}} = 200$ GeV.[1] The primary objective was to measure charge separation under the influence of a magnetic field, referred to as the Chiral Magnetic Effect (CME). These collisions were chosen as an effective strategy to minimize the impact of flow-driven background contributions while investigating the potentially small CME signal.[2,3] Recent studies have also delved into the exploration of nuclear structures through v_2 ratios and v_2-$[p_T]$ correlations in isobar collisions.[4,5] Notably, the deformation parameters differ between the two isobar species, and flow measurements exhibit high sensitivity to these variations. In these collisions, strange and multi-strange hadrons, characterized by their small hadronic cross-section compared to light hadrons, serve as excellent probes for comprehending the initial state anisotropies.

2. Analysis details

In these proceedings, we present the analysis of v_2 for strange and multi-strange hadrons in collisions involving ${}^{96}_{44}\mathrm{Ru}+{}^{96}_{44}\mathrm{Ru}$ and ${}^{96}_{40}\mathrm{Zr}+{}^{96}_{40}\mathrm{Zr}$ at $\sqrt{s_{\mathrm{NN}}} = 200$ GeV, utilizing data collected by the STAR experiment. A comprehensive analysis has been conducted for nearly 650 million events out of 2 billion in each isobar collision system.

The reconstruction of ϕ-mesons is accomplished through the invariant mass technique, specifically via the hadronic decay channel: $\phi \to K^+K^-$ (Branching ratio: 48.9 ± 0.5), within the midrapidity range $|y| < 0.5$.[6] The event mixing technique is employed for estimating the combinatorial background.

Neutral strange particles K_s^0 and $\Lambda(\bar{\Lambda})$ are reconstructed using the invariant mass technique and their weak-decay (V0) topology through the decay channels: $K_s^0 \to \pi^+ + \pi^-$ (B.R. 69.20$\pm$0.05) and $\Lambda \to p + \pi^-$ (B.R. 63.9$\pm$0.5), respectively.[6,7] The multi-strange particle $\Xi^-(\overline{\Xi}^+)$ ($\Lambda + \pi^{\pm}$, B.R. 99.887 ± 0.035) undergoes decay into a charged daughter and a neutral V0 particle (Λ), which subsequently decays into two charged particles.[6] The reconstruction process involves identifying two secondary vertices and applying various topological selections. Combinatorial background for weakly decaying particles is constructed using the rotational background method.[8] The calculation of v_2 for these (multi-)strange hadrons is performed using

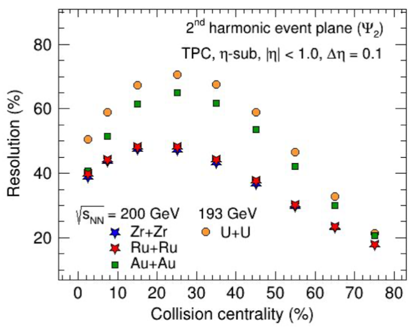

Fig. 1. Event plane resolution as a function of centrality for Ψ_2 in Ru+Ru and Zr+Zr collisions at $\sqrt{s_{\mathrm{NN}}} = 200$ GeV

the η-sub event plane method, with an η gap of 0.1.[7] The event plane angle, Ψ_2 is estimated using the TPC detector in two η windows, $-1.0 < \eta < -0.05$ and

$0.05 > \eta > 1.0$. The calculation of Ψ_2 is done using the equation shown below:

$$\Psi_2 = \frac{1}{2}\tan^{-1}\left(\frac{\Sigma_i w_i sin(2\phi_i)}{\Sigma_i w_i cos(2\phi_i)}\right), \tag{1}$$

where ϕ_i is the azimuthal angle of particle i and w_i is its weight. The resolution of the event plane angle has been calculated using the following equation:

$$R_{sub} = \sqrt{\langle \cos 2(\Psi_2^A - \Psi_2^B)\rangle}, \tag{2}$$

where A and B are the two sub-events, respectively. Notably, both collision systems achieve a maximum event plane resolution of nearly 48% as seen in Fig. 1. We also compare the event plane resolution in isobar collisions with Au+Au collisions at $\sqrt{s_{\rm NN}} = 200$ GeV and U+U collisions at $\sqrt{s_{\rm NN}} = 193$ GeV. The resolution is higher for systems with higher multiplicity and number of participants.

3. Results

The v_2 of strange and multi-strange hadrons, plotted as a function of p_T for minimum bias Ru+Ru and Zr+Zr collisions at $\sqrt{s_{\rm NN}} = 200$ GeV, is depicted in the left panels of Fig.2. A mass ordering is evident at low p_T, while an intermediate p_T range

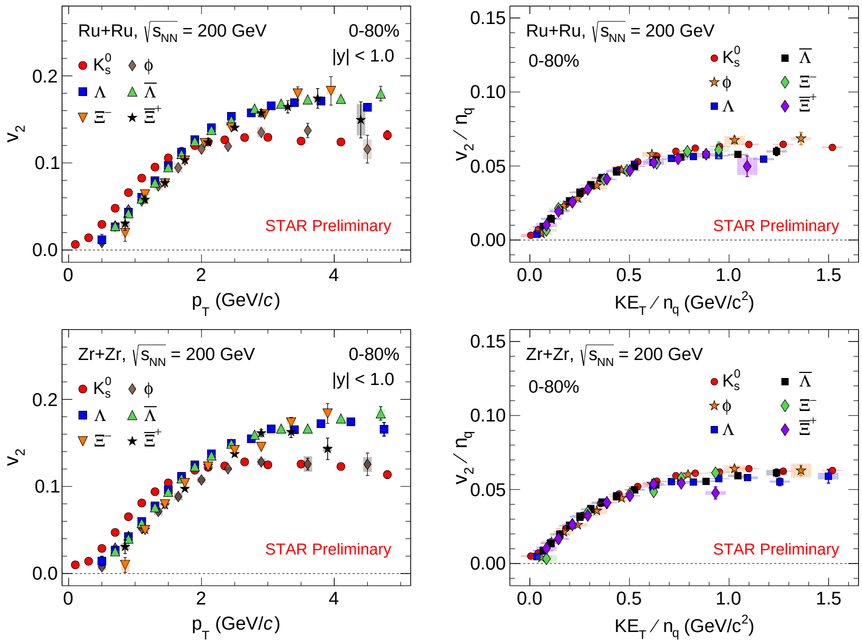

Fig. 2. Left panel: v_2 as a function of p_T for strange hadrons; Right panel: NCQ-scaled v_2 as a function of transverse kinetic energy in Ru+Ru and Zr+Zr collisions at $\sqrt{s_{\rm NN}} = 200$ GeV. The vertical lines and shaded boxes denote statistical and systematic uncertainties, respectively.

reveals a distinct baryon-meson splitting pattern. The v_2 and the transverse kinetic energy ($KE_T = m_T - m_0$) are scaled by the number of constituent quarks (n_q) to test the number of constituent quark (NCQ) scaling. The right panels of Fig.2 illustrate that all particles and their anti-particles exhibit a trend closely adhering to the NCQ scaling within 10%. This observation is indicative of partonic collectivity and the predominance of the quark coalescence mechanism during hadronization.

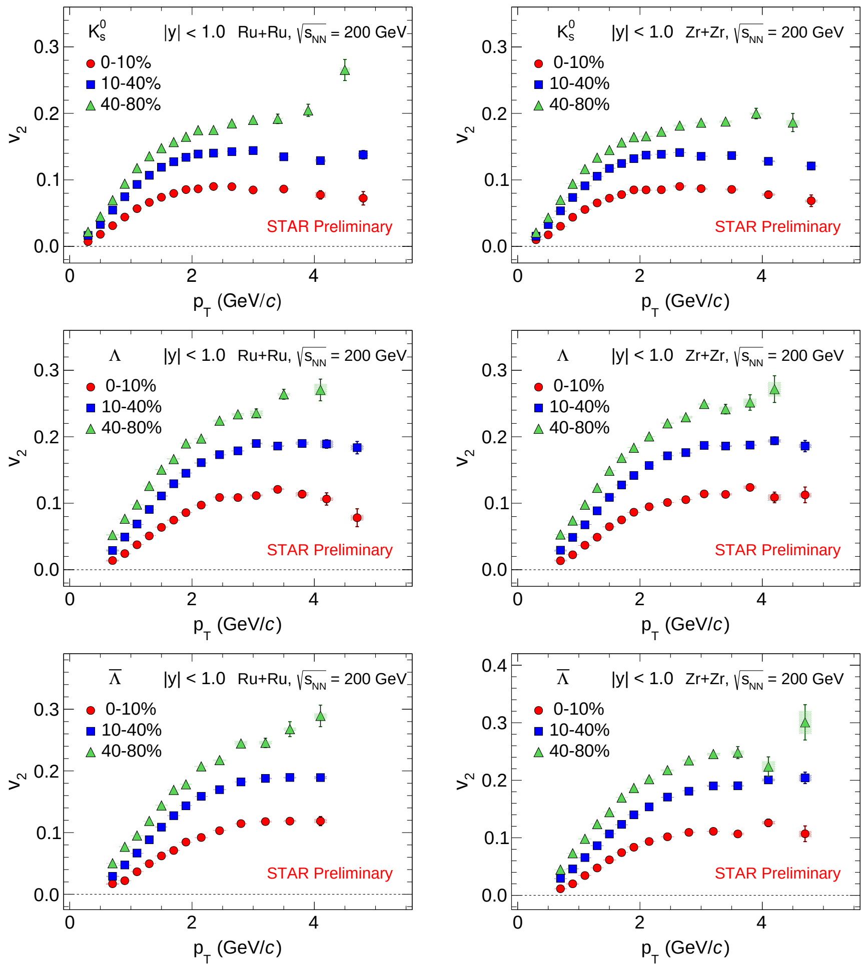

Fig. 3. Left panel: Centrality dependence of v_2 of strange hadrons as a function of p_T in Ru+Ru collisions; Right Panel: Same for Zr+Zr collisions at $\sqrt{s_{\rm NN}}$ = 200 GeV. The vertical lines and shaded boxes denote statistical and systematic uncertainties, respectively.

Figures 3 and 4 show the centrality-dependence of $v_2(p_T)$ of strange (K_s^0, Λ and $\bar{\Lambda}$) as well as multi-strange hadrons (ϕ, Ξ^- and $\overline{\Xi}^+$) in Ru+Ru and Zr+Zr collisions at $\sqrt{s_{\rm NN}}$ = 200 GeV. A pronounced centrality dependence is evident for all studied

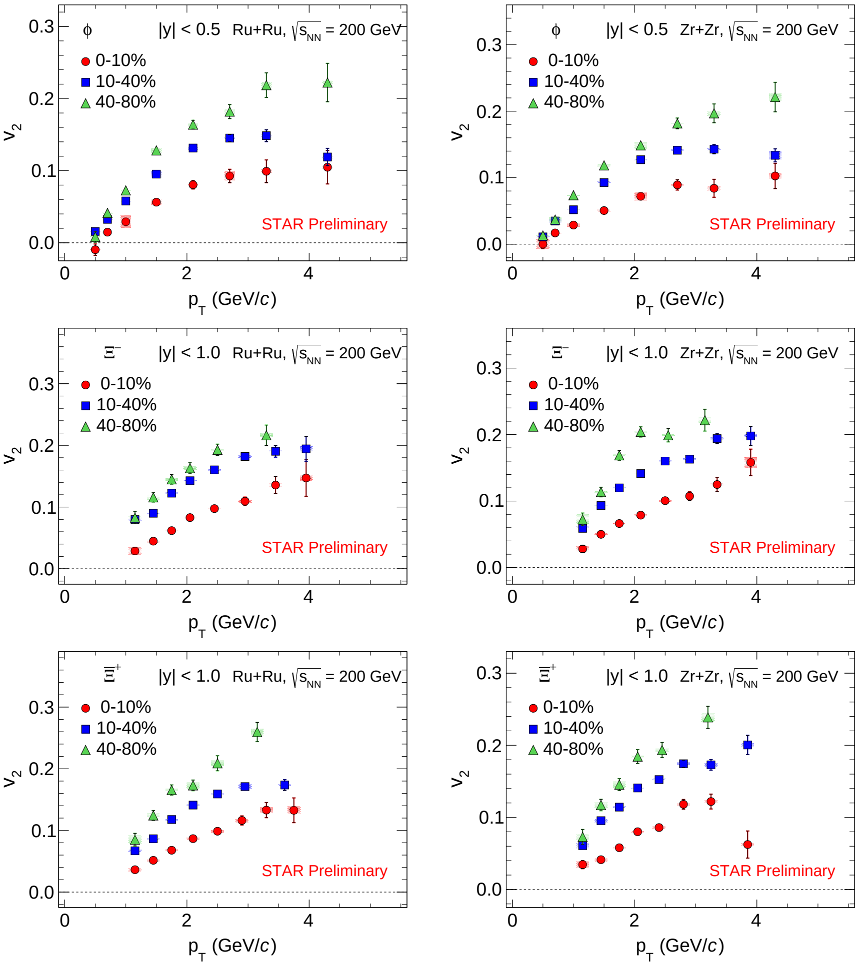

Fig. 4. Left panel: Centrality dependence of v_2 of multi-strange hadrons as a function of p_T in Ru+Ru collisions; Right Panel: Same for Zr+Zr collisions at $\sqrt{s_{\rm NN}} = 200$ GeV. The vertical lines and shaded boxes denote statistical and systematic uncertainties, respectively.

particles in both isobar collision systems. The magnitude of v_2 exhibits a notable increase from central (0-10%) to peripheral (40-80%) collisions, which can be attributed to the larger spatial anisotropy in peripheral collisions in isobar collisions at $\sqrt{s_{\rm NN}} = 200$ GeV.

Additionally, we examine the p_T-integrated v_2 for strange hadrons, as a function of collision centrality in isobar collisions, as illustrated in Fig.5. These ratios deviate by approximately 2% from unity in mid-central collisions, suggesting distinctions in nuclear structure and shape.[1] We investigated the evolution of v_2 with system size by comparing minimum bias $^{63}_{29}$Cu+$^{63}_{29}$Cu, $^{96}_{44}$Ru+$^{96}_{44}$Ru, $^{96}_{40}$Zr+$^{96}_{40}$Zr, $^{197}_{79}$Au+$^{197}_{79}$Au collisions at $\sqrt{s_{\rm NN}} = 200$ GeV, and $^{238}_{92}$U+$^{238}_{92}$U collisions at $\sqrt{s_{\rm NN}} =$

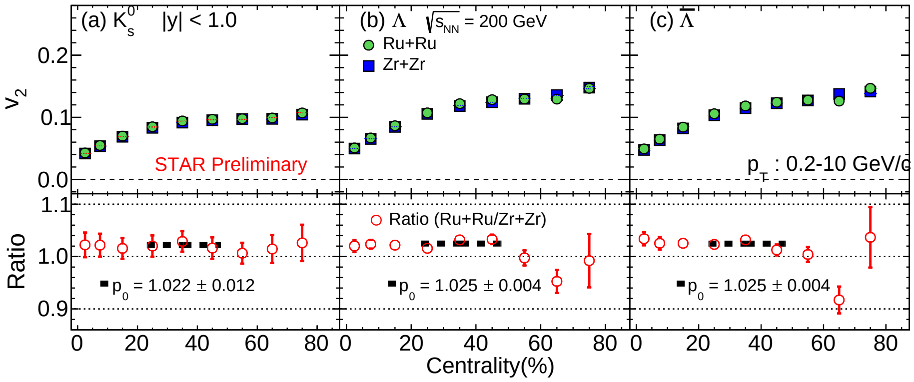

Fig. 5. p_T-integrated v_2 as a function of centrality for K_s^0, Λ, and $\bar{\Lambda}$ in Ru+Ru and Zr+Zr collisions at $\sqrt{s_{\rm NN}}$ = 200 GeV. The vertical lines on the ratio includes statistical and systematic uncertainties. The dotted lines denotes the fitting with a constant.

95 193 GeV.[9–11] Figure 6 illustrates an approximate system size dependence of v_2 for
96 $p_T > 1.8$ GeV/c, based on nuclear size. The v_2 follows the order $v_2^{U+U} > v_2^{Au+Au} > v_2^{Ru+Ru/Zr+Zr} > v2^{Cu+Cu}$.

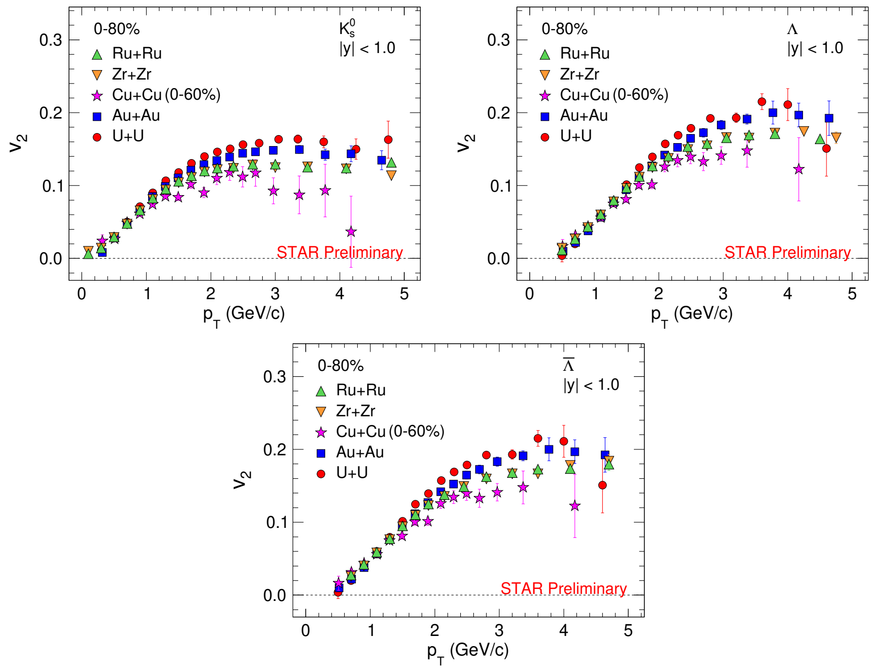

Fig. 6. v_2 of strange hadrons in minimum bias Cu+Cu, Ru+Ru, Zr+Zr, Au+Au collisions at $\sqrt{s_{\rm NN}}$ = 200 GeV and U+U collisions at $\sqrt{s_{\rm NN}}$ = 193 GeV.[9–11]

4. Conclusion

In conclusion, we have presented a comprehensive analysis of the elliptic flow for K_s^0, Λ, $\bar{\Lambda}$, ϕ, Ξ^-, and $\overline{\Xi}^+$ in Ru+Ru and Zr+Zr collisions at $\sqrt{s_{\rm NN}} = 200$ GeV. A prominent mass ordering at low p_T and a baryon-meson splitting at intermediate p_T were observed in both isobar collision systems. All strange particles and their anti-particles exhibit a consistent adherence to the number of constituent quark (NCQ) scaling, indicative of partonic degrees of freedom and a coalescence mechanism during hadronization. The p_T-integrated v_2 ratio of strange hadrons demonstrates a deviation of approximately 2% from unity which can be attributed to the difference in the nuclear structures of Ru and Zr nuclei. Additionally, a system size dependence of v_2 was observed when comparing different collision systems at a similar beam energy. These findings contribute valuable insights into the impact of deformation and collision geometry on the anisotropic flow of particles in relativistic heavy-ion collisions.

References

1. STAR Collaboration (M. S. Abdallah *et. al.*) , Phys. Rev. C **105**, 14901 (2022).
2. D. E. Kharzeev, *Phys. Lett. B* **633**, 260-264 (2006).
3. D. E. Kharzeev, J. Liao, *Nature Rev. Phys.* **3**, 55-63 (2021).
4. C. Zhang and J. Jia, *Phys. Rev. Lett.* **128**, 022301 (2022).
5. J. Jia, S. Huang, and C. Zhang, *Phys. Rev. C* **105**, 014906 (2022).
6. Particle Data Group, *Chinese Phys. C* **38**, 090001 (2014).
7. STAR Collaboration (L. Adamczyk *et. al.*), Phys. Rev. C **88**, 014902 (2013).
8. STAR Collaboration, (J. Adams *et. al.*) Phys. Rev. Lett. **95**, 122301 (2005).
9. STAR Collaboration (B. I. Abelev *et al.*), Phys. Rev. C **81**, 044902 (2010).
10. STAR Collaboration (B. I. Abelev *et al.*), Phys. Rev. C **77**, 054901 (2008).
11. STAR Collaboration (M. S. Abdallah *et al.*), Phys. Rev. C **103**, 064907 (2021).